IPACK2023-113883

DEVELOPMENT OF THERMAL METROLOGY STANDARDS FOR EXPERIMENTAL CHARACTERIZATION OF THERMAL RESISTANCE FOR SINGLE-PHASE LIQUID COLD PLATES

Alfonso Ortega 1,†,*, Victor A. Martinez 1,†, Carol Caceres 1,†, Ali Heydari², Uschas Chowdhury²

¹Villanova University, Villanova, PA ²NVIDIA Corporation, Santa Clara, CA

ABSTRACT

Over the last decade, a significant number of investigations have been performed to develop and optimize cold plates for direct-to-chip cooling with cold plates attached to processor packages. Many investigations have reported computational simulations using commercially available CFD tools that are compared to experimental data. Generally, the simulations and experimental data are in qualitative agreement but often not in quantitative agreement. The computational simulations are used for thermal and hydraulic characterization of these cold plates and are used to perform parametric analysis to address the cold plate's optimal design. Unfortunately, the experimental characterizations have high uncertainty due to lack of proper attention to the basic measurements, particularly of temperature. Extensive experimental evaluations reported in this paper will be used to demonstrate the frequent errors in experimental thermal measurements used in forming the defined thermal resistance and the experimental artifacts during testing that lead to unacceptable inconsistency and uncertainty in the reported results. By comparing experimental thermal data such as the temperature at multiple points on the processor lid, and using that data to extract a meaningful measure of thermal resistance, it will be shown that the data uncertainty and inconsistency is primarily due to three factors: (1.) inconsistency in the thermal boundary condition supplied by the TTV to the cold plate; (2.) errors in the measurement and interpretation of the surface temperature of a solid surface, such as the heated lid surface or the base of the cold plate, and (3.) errors introduced by improper contact between cold plate and TTV. A standard thermal test vehicle (STTV) was designed and used to provide reproducible thermal boundary conditions to the cold plate. An uncertainty analysis was performed in order to discriminate between the sources of inconsistencies in the reporting of thermal resistance, including parameters such as mechanical

load distribution, methods for measuring the cold plate base, and TTV surface temperatures.

Keywords: Metrology, Heat Sink Cold Plate, Case Temperature

NOMENCLATURE

\boldsymbol{A}	Area [m ²]	
H	Height, m	
k	Thermal Conductivity [Wm ⁻¹ K ⁻¹]	
LMTD	Logarithmic Mean Temperature Difference [K]	
Q	Heat Flow [W]	
$q^{\prime\prime}$	Heat Flux [Wm ⁻²]	
R	Thermal Resistance [KW ⁻¹]	
$R^{\prime\prime}$	Unit Thermal Resistance [Km ² W ⁻¹]	
T	Temperature [K]	
ΔT	Temperature Difference [K]	
U	Uncertainty	
U	Overall Heat Transfer Coefficient [Wm ⁻² K ⁻¹]	
W	Width, m	
Greek letters		
σ	Standard deviation	
ϕ	Aspect ratio, [-]	
Non-Dimensional groups		
Bi	Biot number	
Supersci	ripts and subscripts	
Av	Based on the average temperature	
b	Bulk Value	
c	Case	
cp	Cold Plate	
Ct	Based on the center temperature	
Fo	Based on the extrapolated temperature following	
	Fourier's Law	
g	Thermal Adhesive Compound	
HA	Heated Area of the STTV	
in	inlet	

 $^{^{\}dagger}\text{Joint first authors}$

^{*}Corresponding author: alfonso.ortega@villanova.edu
Documentation for asmeconf.cls: Version 1.34, July 28, 2023.

m Meanout outlets Surface

1. INTRODUCTION

Direct to chip cooling for CPUs and GPUs has been extensively studied to manage the heat dissipation. Cold plates with different extended surface elements, flow patterns, and geometrical parameters have been developed and generally offer an efficient heat removal solution for high-power devices compared to air cooling. The most common cold plates utilize parallel straight fins with flow either parallel to the fin passage or normal to the fin passage. In previous research by this team, Ortega et al. [1] evaluated the performance limits of parallel flow straight fin cold plates. Kisitu and Ortega [2] have compared the performance of parallel flow configurations with impinging or split flow configurations. The primary performance metrics documented and evaluated have been the overall base to inlet thermal resistance and the pressure drop.

Thermal resistance is the most common metric used to evaluate the thermal performance of cold plates although as noted in Ortega et al. [1] it is neither the best nor the most robust performance parameter for such characterizations. The thermal resistance historically was defined in such a way that it can be inserted into the overall thermal resistance representation of an electronic package structure. As such, it is a defined quantity, given most generally as:

$$R = \frac{\Delta T}{Q} \tag{1}$$

The apparent simplicity of the definition has led to its widespread usage, but unfortunately, also to proliferation of inconsistent and incorrect application. Ortega et al. [1] outlined an approach that is consistent with the widely known theories developed for compact heat exchangers, with the underlying assumption that a cold plate is in fact a compact heat exchanger. In the definition of Eq. (1) the major inconsistencies arise from the definition of ΔT . If as in heat exchanger theory, the heated surface is assumed to be isothermal, with temperature T_s and with fluid inlet mean temperature $T_{m,in}$ and outlet mean temperature, $T_{m,out}$, then:

$$Q = UA_s \cdot LMTD \tag{2}$$

where,

$$LMTD = \frac{(T_s - T_{m,out}) - (T_s - T_{m,in})}{\ln\left(\frac{T_s - T_{m,out}}{T_s - T_{m,in}}\right)}$$
(3)

The consistent definition for thermal resistance would then be:

$$R_{LMTD} = \frac{1}{UA_s} = \frac{LMTD}{O} \tag{4}$$

However, this is not the definition that has been popularized in the electronics cooling literature. The common definition is:

$$R = \frac{T_s - T_{m,in}}{O} \tag{5}$$

To achieve consistency both theoretically and experimentally using this definition, several important points needs to be emphasized:

- Most thermal test vehicles (TTVs) designed to characterize cold plates do not provide either a uniform heat flux nor a uniform temperature boundary condition at the base of the TIM which adhered to the base of the cold plate
- The assumption that the extended surfaces (fins) in the cold plate are isothermal is false—the lack of isothermally along the perimeter can be corrected by introducing fin effectiveness

This does not correct for lack of isothermally in the streamwise direction. Hence, when applying either Eq. (4) or (5) to define R, there is ambiguity in the definition of the surface temperature because neither the cold plate base nor the electronic component lid or case are isothermal. This error between experiment and numerical simulation is not an experimental measurement error, rather it is an error due to poor control of thermal boundary conditions.

The thermal resistance based on the case or lid temperature necessarily includes the TIM resistance and the cold plate overall resistance. If the TIM thermal resistance is included, uncertainties must include those of the TIM and repeatability must account for the TIM application procedure and testing parameters that affect TIM performance such as mechanical load. TIMs can be categorized as thermal greases, phase-change materials, gels, thermal pads, and thermal pastes. Based on these groups, the TIM material selection and the experiment test condition are crucial to achieving consistency and repeatability in performing comparative studies between cooling technologies. Zhao et al. [3] studied parameters such as surface roughness, temperature, and pressure, affecting thermal resistance behavior. The author pointed out that phase-change materials (PCMs) thermal resistance are not sensitive to roughness but highly dependent on temperature and pressure. PADs achieve good performance when the loading pressure is significant, which can affect the mechanical integrity of the chip [4]. Ramakrishna and Prabhu [5] presented a complete and highly detailed review paper about TIMs challenges and the horizon these materials will target.

Thermal resistance measurements on the cold plate introduce other ambiguities based on whether it is defined in terms of the case temperature or the cold plate base temperature. In the first case, the TIM thermal resistance will be included, and the lack of standard procedures for performing this measurement is critical. Measurement of the surface temperature of the package lid or case with a point sensor introduces at least two errors that are unavoidable, the sensor error, and the error introduced on the surface temperature by the presence of the sensor. Moffat [6] refers to these as the Zeroth and the First Order uncertainties. Therefore, suitable techniques to measure these surfaces are required. Azar and Kaveh [7] mentioned that in the case of using

thermocouples, the wire selected must be 36 gauge and type-K as it offers the lowest errors by heat conduction. However type-K thermocouples are challenging to solder to a highly conductive surface. The authors point out that type-T thermocouples can induce a high error because they are composed of highly conductive material, however they are easier to solder to the surface. Kozarek [8] commented that obtaining R_{jc} (Thermal Resistance from junction-to-case) presents challenges in the case temperature measurement. Kozarek, demonstrated that standards available such as MIL-883C [9], JEDEC [10], and SEMI [11] to determine R_{ic} gave erroneous surface temperatures. These standards are designed to define the R_{jc} using a liquid cold plate as a heat sink, and the case temperature is measured by a fluorOptic temperature probe (Kozarek [8] implementation) inserted in a thru-hole in the center of the cold plate. The same methodology cannot be applied to evaluate cold plate thermal performance since the case temperature measurement is intrusive and will interfere with the flow distribution in the cold plate. The Open Compute Project (OCP) [12] initiated an effort on cold plate development and qualification but has not included recommendations for experimental thermal measurements.

Because of the lack of accepted measurement standards for characterization of cold plate thermal resistance, this work aims to clarify the errors introduced by improper measurement and interpretation of case temperature with thermocouples. In particular, we will examine the sensitivity of the case temperature measurement to thermocouple placement procedures with recommendations for best practices based on a standard TTV design used for this study.

2. EXPERIMENTAL METHODS

2.1 Experimental Apparatus

In order to characterize the cold plate, the flow loop shown in Fig. 1 was constructed to deliver coolant (25vol.% Propylene Glycol) at a controlled pressure, temperature, and flow rate. The coolant is pumped by a positive displacement gear pump (Diener, Extreme 4000). Downstream of the reservoir, the coolant is pumped through a trimmer heat exchanger, where its temperature is adjusted to reach the desired inlet temperature. After exiting the heat exchanger, the coolant flows through the electromagnetic flowmeter (IFM SM6004) and enters the test section. Downstream of the test section, the coolant passes through the primary heat exchanger rejecting the heat absorbed in the previous stage and completing the loop by returning to the reservoir.

2.2 Standard Thermal Test Vehicle and Cold Plate

The standard thermal test vehicle shown in Fig. 2 was engineered to attenuate the three-dimensional effects produced by the change in geometry from the heat source (cylindrical cartridge heaters) to the heat-flux-meter bar, providing a one-dimensional heat flux to the cold plate. To measure the heat flux delivered to the cold plate, four vertically installed Chromel-Alumel (Type-K) thermocouples with a diameter of 0.3 mm were placed into 1 mm bore holes that were machined in the heat-flux-meter bar. A numerical analysis was performed to validate the locations of

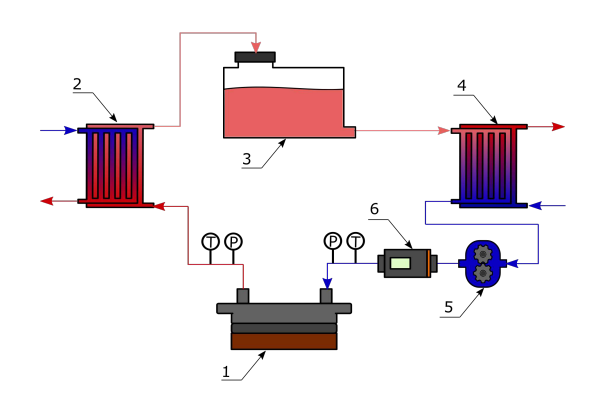


FIGURE 1: SCHEMATIC OF FLOW LOOP. 1) TEST SECTION, 2) PRIMARY HEAT EXCHANGER, 3) COOLANT RESERVOIR, 4) TRIMMER HEAT EXCHANGER, 5) GEAR PUMP, AND 6) ELECTROMAGNETIC FLOWMETER.

the thermocouples and the degree of agreement with the onedimensional conduction assumption used to determine the heat flux. For the three-dimensional finite difference analysis, an unstructured mesh of 837,327 elements was used to solve the steady-state energy equation that governs the heat transfer process. The boundary conditions listed in table 1 correspond to the experimental conditions implemented on the test carried out to validate the thermal performance of the STTV. The validation experiment was performed by placing a microchannel cold plate onto the STTV to keep its heated area isothermal. The cartridge heaters were powered with 1000 W with 2 LPM volumetric coolant flow rate supplied to the cold plate. The inlet temperature of the coolant was set at 32°C, obtaining a thermal resistance of 0.0198±0.0021 Wm⁻¹K⁻¹ whose corresponding unit thermal resistance is the value implemented as a boundary condition on the top surface of the STTV.

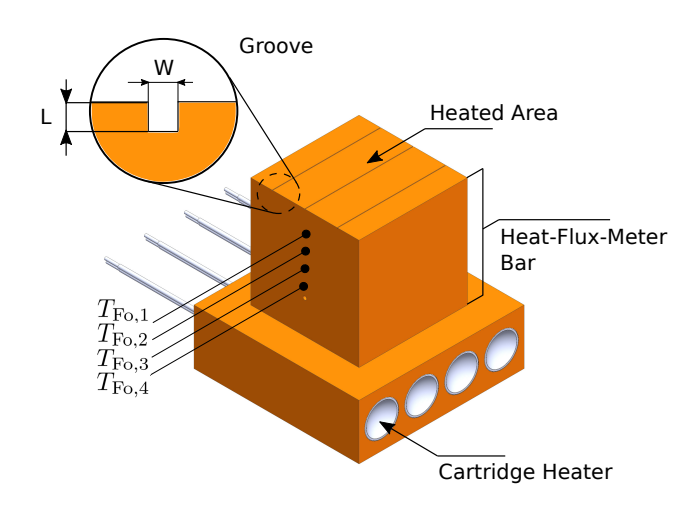


FIGURE 2: STANDARD THERMAL TEST VEHICLE.

The results shown in Fig. 2 show agreement between the numerical and the experimental measurements of the center line

temperature. The region where the thermocouples were placed in the heat-flux-meter bar clearly shows a linear temperature distribution and is not influenced by two-dimensional heat conduction effects.

TABLE 1: BOUNDARY CONDITION IMPLEMENTED ON THE NU-MERICAL ANALYSIS.

Location	Boundary condition
Top Surface	$R''=4.95\times10^{-5} \text{ m}^2\text{KW}^{-1}$ $T_b=35.21^{\circ}\text{C}$
Vertical Surfaces	$\partial T/\partial \hat{n}=0 \text{ KW}^{-1}$
Thru-Hole Curved Surfaces	q''=65784.175 Wm ⁻²

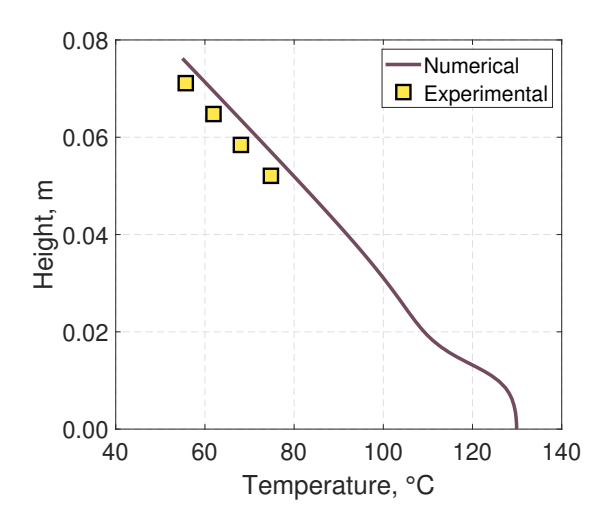


FIGURE 3: NUMERICAL AND EXPERIMENTAL RESULTS FOR THE CENTERLINE TEMPERATURE OF THE STTV IN THE VERTICAL DIRECTION.

A commercial microchannel cold plate previously documented in Ortega et al. [1] was used to evaluate thermal resistance measurements, with parametric variations in the thermocouple placement procedures. The cold plate is a side-in, side-out single-phase microchannel heat sink whose geometrical features are shown in Table 2.

TABLE 2: COLD PLATE GEOMETRICAL CONFIGURATION.

Channel width, mm	0.2
Channel height, mm	4
Channel length, mm	43
Number of channels	120
Fin thickness, mm	0.2

2.3 Experiment Procedure

The test section of the flow loop (Fig. 4) includes the the cold plate, the STTV, and the thermal interface material (TIM) used to guarantee the thermal contact between pieces. The cold plate was secured to the heated area using four spring-loaded bolts that applied a specific loading pressure. The springs have been experimentally characterized by performing compression tests using an electromechanical testing machine (MTS Criterion

Model 41). From the results shown in Fig. 5, the average spring constant was 10.205 ± 0.005 kN/m. To study the influence of thermal contact on the thermal characterization of cold plates, two loading pressure levels (10 PSI and 15 PSI) and TIM (Honeywell PTM 7950 and Artic Silver grease MX-4) were investigated.

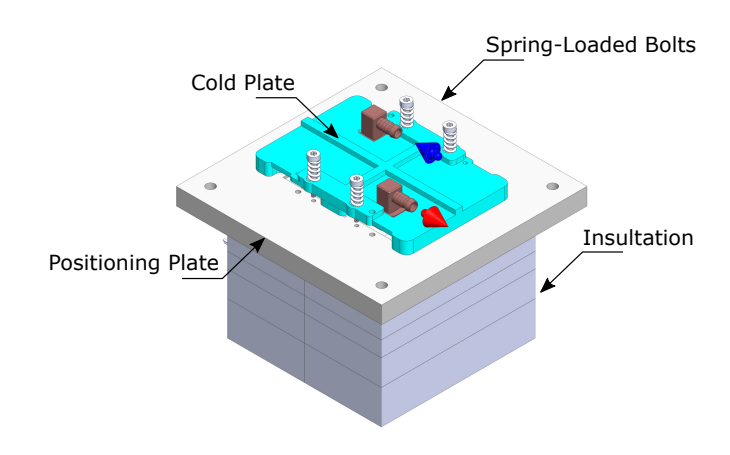


FIGURE 4: TEST SECTION OF THE RIG.

The volumetric flow rate was varied from 1 LPM to 4 LPM. Under steady-state conditions, three inlet temperatures were considered: 22°C, 32°C, and 42°C. To measure the temperatures at the inlet and the outlet of the test section, 3.2 mm diameter type-K thermocouple probes were inserted into the copper tubing connected to the cold plate. The temperature of the base of the cold plate was registered by placing three butt-welded type-K thermocouples (0.08 mm diameter) and the distance between grooves is 15 mm (Fig. 6). These thermocouples were diagonally installed (with respect to the flow stream direction) to capture the manifold's effects on the channels' flow distribution. Similarly, the case temperature (i.e. the top surface of STTV (2)) was measured with three butt-welded type-K thermocouples embedded in grooves machined on the STTV surface following the same pattern used in Fig. 6.

The influence of the thermocouple placement on the case temperature measurements was studied by setting two groove depth levels (0.46 mm and 1.09 mm) for a fixed width (0.53 mm), obtaining two aspect ratios ($\phi = L/W$): 0.9 and 2.1. Since the thermocouple is not large enough to fill the groove, thermal adhesive compound was applied to place the thermocouples to the corresponding surface and avoid air voids that perturb the temperature readings. Furthermore, the thermal adhesive compound (GENNEL G109) was chosen over epoxy and soldering because it can be easily reworked and allows thermocouple replacement. The dimensions of the grooves were measured with a digital microscope (Celestron, 5 MP Digital Microscope Pro), and processing the images in the open-source software ImageJ Fiji.

A KEYSIGHT N8762A DC power supply unit was used to power the cartridge heaters at the bottom of the TTV. For all the experiments performed in this study, 1000 W nominal electrical

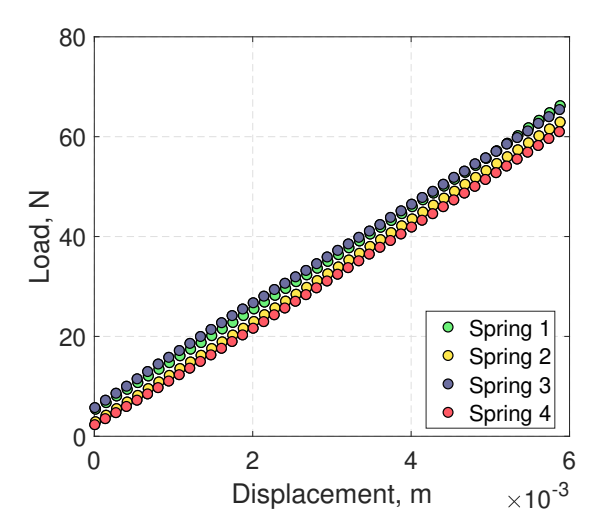


FIGURE 5: LOAD-DISPLACEMENT CURVES OBTAINED FROM THE COMPRESSION TESTS ON THE SPRINGS.

power was supplied. Using a one-dimensional conduction model, the heat flux that reached the cold plate was determined using the thermocouples placed in the heat-flux-meter bar. All the thermocouples were connected to a data acquisition system (NI cDAQ-9174) referenced to an ice bath.

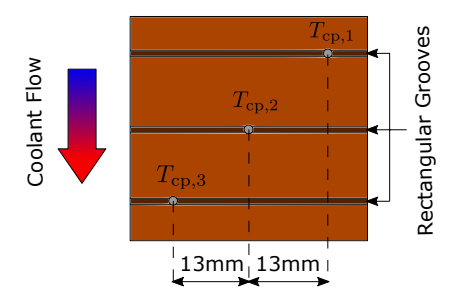


FIGURE 6: SCHEMATIC OF THE THERMOCOUPLE PLACEMENT.

3. DATA REDUCTION

3.1 Thermal Resistance

The definition of the thermal resistance of the system cold plate/TIM is given by Eq. (6),

$$R = \frac{T_c - T_{in}}{Q} \tag{6}$$

where Q the heat flow provided by the STTV, T_{in} corresponds to the inlet temperature of the coolant and T_c is the case temperature, which in these experiments is the surface of the STTV used as seen in Fig. 2. Depending on the method used to determine the case temperature, three different thermal resistances were defined. First, the thermal resistance is calculated based on the centerline case temperature, defined as the temperature measured on the center of the heated area of the STTV (Eq. (7)).

$$R_{Ct} = \frac{T_{HA,2} - T_{in}}{Q} \tag{7}$$

Second, the thermal resistance is computed with the case temperature defined as the average temperature of the heated area of the STTV (Eq. (8)).

$$R_{Av} = \frac{\overline{T}_{HA} - T_{in}}{O} \tag{8}$$

where \overline{T}_{HA} is the arithmetic average temperature.Lastly, relying on the one-dimensional conduction assumption made along the heat-flux-meter bar, the case temperature was defined as the temperature that is extrapolated using the linear temperature distribution ($T_{Fo,1}$ in Fig. 2) to the heated area. Hence,

$$R_{Fo} = \frac{\overline{T}_{c,Fo} - T_{in}}{O} \tag{9}$$

where

$$T_{c,Fo} = T_{Fo,1} - \frac{Q\Delta y}{kA} \tag{10}$$

where Δy corresponds to the distance between the heated area of the STTV to the nearest thermocouple installed in the HFMB ($T_{Fo,1}$). The heat flow was determined assuming one-dimensional conduction on the heat-flux-meter bar, thus

$$Q = -kA \frac{\partial T}{\partial y} \tag{11}$$

where the temperature gradient was obtained from a linear regression applied to the set of centerline temperature measurements. The thermal conductivity was considered constant with respect to the temperature using the value provided by Lees et al. [13] and published at the NIST Thermodynamics Research Center $(382.836\pm38.2836~\mathrm{Wm}^{-1}\mathrm{K}^{-1})$.

3.2 Uncertainty Analysis

An uncertainty analysis (Eq. (12)) was performed using the method proposed by R.J. Moffat [6]. The corresponding expressions of the sensitivity coefficients $(\partial y/\partial x_j)$ are listed in the appendix for the thermal resistances, the heat flow, and the case temperature extrapolated following Fourier's Law (tables 3-5).

$$U_{y} = \left(\sum \left(\frac{\partial y}{\partial x_{j}} \cdot U_{x_{j}}\right)^{2}\right)^{1/2} \tag{12}$$

4. RESULTS AND DISCUSSION

From the series of experiments performed with a groove aspect ratio ϕ =0.9 machined in the heated area of the STTV, the results in Fig. 7 show that for constant loading pressure, TIM, and inlet coolant temperature, the different definitions of the thermal resistance can lead to an average discrepancy of 42.9%. This level of disagreement was observed between R_{Fo} and R_{Av} . The STTV surface temperature found by extrapolation of the linear temperature profile is assumed to be the "true" temperature. Placing thermocouples on the heated surface of the STVV introduces a significant error in the case temperature measurements, which

negatively impacts the thermal resistance determination. However, R_{Fo} presents larger error bars, which can be attributed to the extrapolation of the case temperature.

Regarding the differences between using the averaged case temperature or the center temperature, the results show an average discrepancy of 3.3%, which validates the isothermal heated area assumption implicit in the one-dimensional conduction hypothesis.

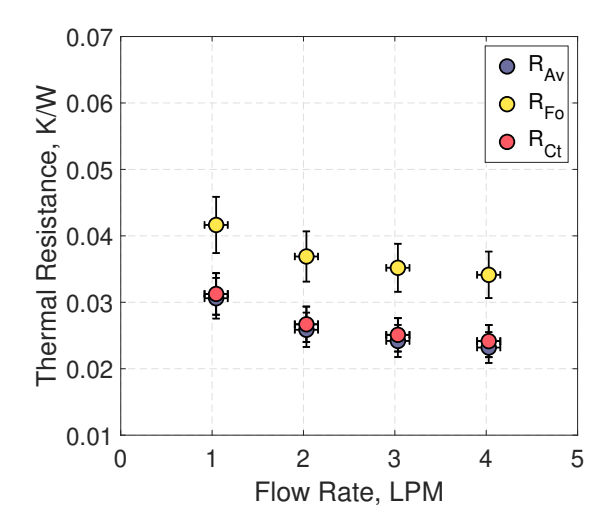


FIGURE 7: DEPENDENCY OF THE THERMAL RESISTANCE OF THE COLD PLATE/TIM SYSTEM ON ITS DEFINITION FOR ϕ =0.9. EXPERIMENTS PERFORMED USING GREASE, APPLYING 15 PSI JOINING PRESSURE, AND PROVIDING COOLANT AT 32°C.

To investigate the impact of the depth of the thermocouple groove in the measured case temperature, deeper grooves were machined on the heated surface of the STTV, resulting in an aspect ratio ϕ =2.1. When tested under the same conditions as before, the thermal resistance of the cold plate/TIM system showed better agreement, as shown in Fig. 8. On average, the discrepancy between R_{Fo} and R_{Av} was 9.0%. The improvement in the measurement of the true undisturbed surface temperature by using a deeper groove is more likely as a result of compensating for the surface temperature depression in a shallow groove, by embedding the thermocouple in a region that it has a higher temperature.

4.1 Numerical Simulation of Thermocouple Placement

The effect of placing the thermocouple on the heated surface area of the STTV was numerically studied as a function of the aspect ratio of the groove. The two-dimensional computational domain was discretized using a non-uniform mesh of 9066 elements, setting a 1000 W heat flow on the bottom, and the top surface boundary condition exposed in table 1. As can be seen in Fig. 9, by introducing the thermocouple in the groove, a temperature drop is introduced to the area surrounding the thermocouple, which can mainly be explained by the lower thermal conductivity of the thermal adhesive compound ($k_g = 1.2 \text{ Wm}^{-1} \text{K}^{-1}$), and the groove's geometry itself.

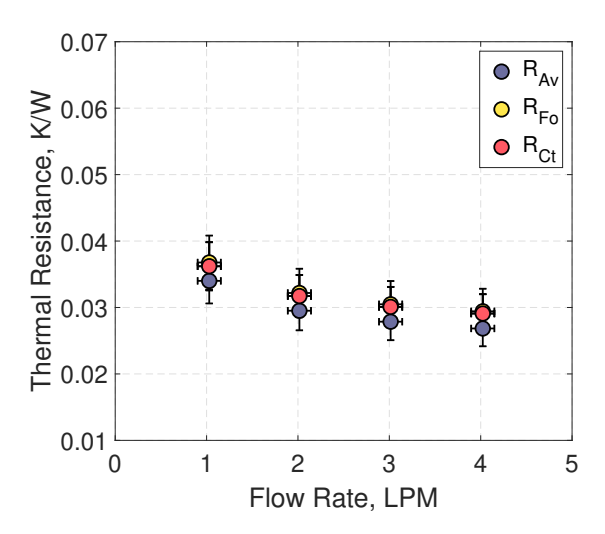


FIGURE 8: DEPENDENCY OF THE THERMAL RESISTANCE OF THE COLD PLATE/TIM SYSTEM ON ITS DEFINITION FOR ϕ =2.1. EXPERIMENTS WERE PERFORMED USING GREASE, APPLYING 15 PSI JOINING PRESSURE, AND PROVIDING COOLANT AT 32°C.

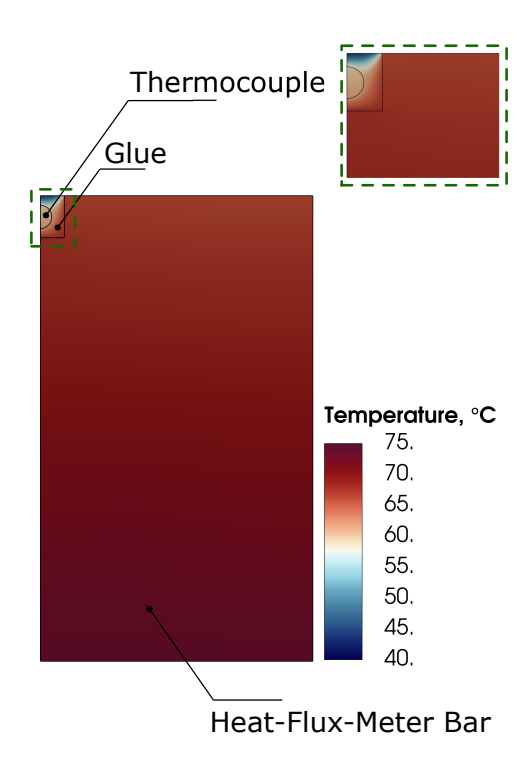


FIGURE 9: TEMPERATURE DISTRIBUTION OF THE REGION SURROUNDING A GROOVE OF ASPECT RATIO L/W=0.9 IN THE HFMB FOR A BI=0.9.

Extending the numerical analysis, the error of the case temperature measurement was examined as a function of the aspect ratio of the groove ϕ in the range between 0.7 and 2.1. The measurement error was defined numerically as the difference between the average temperature of the thermocouple T_m and the average temperature of the top boundary condition in the computational domain T_c , where this temperature was determined by performing a simulation with no thermocouple or groove. In Fig.10, the

results obtained for the error of the case temperature measurement are shown for three Biot numbers defined in termsa of the width of the groove (Eq.13).

$$Bi = \frac{hW_{\text{groove}}}{k_g} = \frac{W_{\text{groove}}}{R''k_g} \tag{13}$$

where the unit thermal resistance is given by the Eq. 14 and shown in table 1

$$R^{\prime\prime} = R \cdot A \tag{14}$$

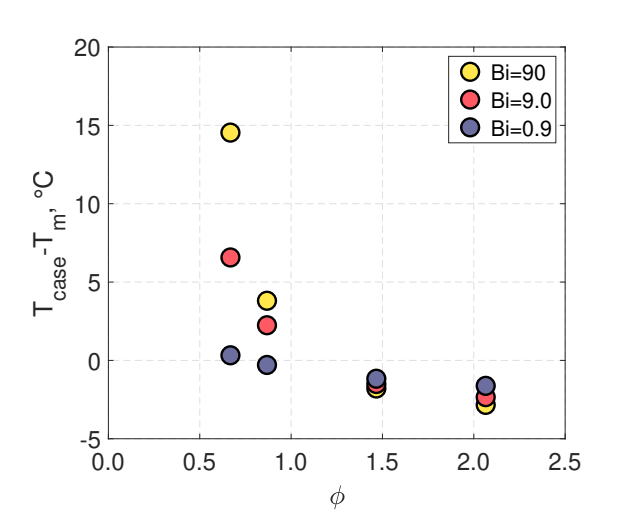


FIGURE 10: TEMPERATURE DISTRIBUTION OF THE REGION SUR-ROUNDING THE GROOVES OF THE HFMB.

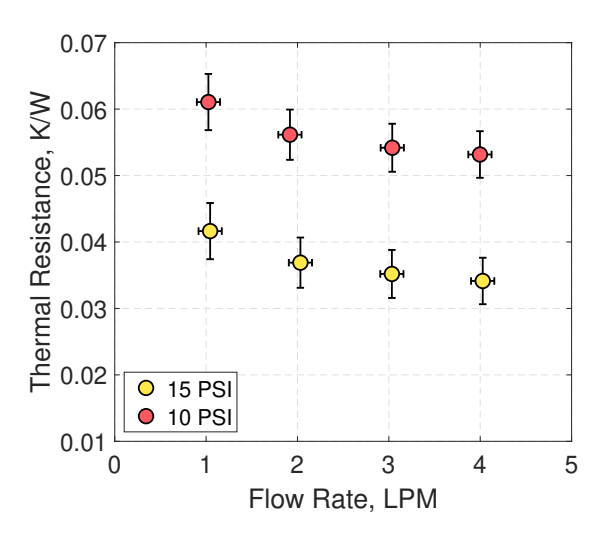


FIGURE 11: THERMAL RESISTANCE OF THE COLD PLATE/TIM SYSTEM FOR TWO JOINING PRESSURE LEVELS. EXPERIMENTS PERFORMED WITH GREASE AND PROVIDING COOLANT AT 32°C.

As can be seen, the temperature perturbation exhibited in the groove due to the insertion of the thermocouple can be rectified by increasing the depth of the groove for all the Biot numbers studied, reaching an ideal aspect ratio for which $T_c - T_m$ goes to zero. However, the temperature measured with the ideal aspect

ratio does not correspond to the actual case temperature but only a rectified value. Furthermore, the optimized aspect ratio that leads to a non-error case temperature measurement varied with the Biot number. This means that any given cold plate, coolant flow rate, TIM, or thermal adhesive compound would require a different groove aspect ratio to rectify the case temperature measurement, which can clearly be seen in Fig. 10. For the present study the Biot number was ranging from 4.2 to 6.0.

4.2 Effect of Loading Pressure

To ensure thermal contact between the cold plate and the STTV, grease and PTM were used as TIMs; their thermal resistance depends on the loading pressure [14], among other factors. The sensitivity of the thermal resistance of the system cold plate/TIM regarding the loading pressure is shown in Fig. 11 where no effect related to the thermocouple placement was considered since those magnitudes correspond to the thermal resistances obtained from Eq. 9. Although both data groups follow the same trend, the thermal resistance of the system loaded with 10 PSI is 34.2% higher than the case with 15 PSI. It is important to note that for both cases, the same amount of grease was applied, which was achieved with a tool that removes the excess material leaving constant cross-section area stripes (2.4 mm × 2.4 mm) on the heated surface of the STTV.

4.3 Effect of Coolant Temperature

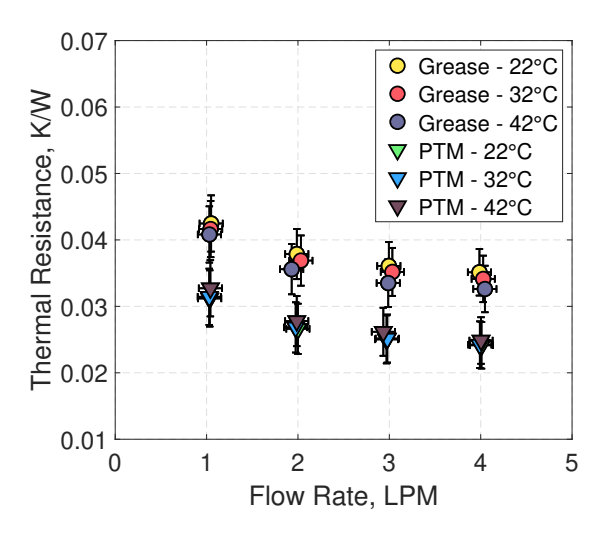


FIGURE 12: EFFECT OF THE INLET COOLANT TEMPERATURE ON THE THERMAL RESISTANCE OF THE COLD PLATE/TIM SYSTEM. EXPERIMENTS WERE CARRIED OUT WITH GREASE AND PTM AT CONSTANT JOINING PRESSURE (15 PSI).

Regarding the effect of the coolant inlet temperature, no major differences were observed either the grease or the PTM, as can be seen in Fig. 12. In fact, the set of curves corresponding to the experiments performed with grease overlap each other, and the minor discrepancies can be explained by the trend to flow of the grease due to the decreased viscosity at higher temperatures. The magnitude of the difference is 6.05% on average, between the cases where $T_{in}=22^\circ$ and $T_{in}=42^\circ$ C. Similar results were

found for the PTM, which had a 4.2% difference between the same two temperatures. Since both the grease and the PTM were well-behaved with respect to the coolant inlet temperature in the range between 22°C and 42°C, a consistent characterization can be carried out using either grease or PTM. However, on average, the PTM has shown a 36.6% lower thermal resistance. It is worthy to remark that the thermal resistance estimated using Eq. 9, was not subject to thermocouple placement effects.

5. CONCLUSIONS

- 1. An experimental procedure for the thermal characterization of single-phase cold plates was developed. The methodology has considered different definitions of the thermal resistance commonly applied in the literature, and the sources of error that affect its magnitude, quantifying their influence on this parameter
- 2. A standard thermal test vehicle that delivers a thermally measurable heat flux to the cold plate was designed. By attenuating the three-dimensional effects introduced by the cylindrical cartridge heaters, the device allows applying a one-dimensional conduction model to determine the case temperature without needing thermocouples on the heated area.
- 3. The method of installing a thermocouple on the lid to measure the case temperature was experimentally and numerically studied as a function of the aspect ratio of the groove used to install it. The results suggest that the case temperature directly measured with a thermocouple presents a significant uncertainty that depends on the Biot number and the aspect ratio of the groove, where the latter can be used to rectify the thermocouple measurements
- 4. Both PTM and grease were used to characterize the thermal resistance of the cold plate. While PTM exhibits lower thermal resistances than grease, both were unaffected by the coolant inlet temperature within the range studied. Conversely, the joining pressure has shown a significant effect on the thermal resistance of the system cold plate/TIM being 15 PSI, the magnitude that provides lower results for grease

ACKNOWLEDGMENT

This material is based upon the work supported by the National Science Foundation Center for Energy Smart Electronic System (ES2) under the Grant No. IIP 1738782. Any opinions, findings, and conclusions, or recommendations expressed in this material are those of the author(s) and do not necessarily reflect the views of the National Science Foundation.

REFERENCES

[1] Ortega, Alfonso, Caceres, Carol, Uras, Umut, Kisitu, Deogratius, Chowdhury, Uschas, Radmard, Vahideh and Heydari, Ali. "Determination of the Thermal Performance Limits for Single Phase Liquid Cooling Using an Improved Effectiveness-NTU Cold Plate Model." *International Electronic Packaging Technical Conference and Exhibition*, Vol.

- 86557: p. V001T01A008. 2022. American Society of Mechanical Engineers.
- [2] Kisitu, Deogratius and Ortega, Alfonso. "Thermal-Hydraulic Analytical Models of Split-Flow Microchannel Liquid-Cooled Cold Plates With Flow Impingement." *International Electronic Packaging Technical Conference and Exhibition*, Vol. 85505: p. V001T02A015. 2021. American Society of Mechanical Engineers.
- [3] Zhao, Jian-Wei, Zhao, Rui, Huo, Yan-Kai and Cheng, Wen-Long. "Effects of surface roughness, temperature and pressure on interface thermal resistance of thermal interface materials." *International Journal of Heat and Mass Transfer* Vol. 140 (2019): pp. 705–716.
- [4] Bahrami, Majid, Yovanovich, M Michael and Culham, J Richard. "Thermal contact resistance at low contact pressure: Effect of elastic deformation." *International Journal* of Heat and Mass Transfer Vol. 48 No. 16 (2005): pp. 3284–3293.
- [5] Pathumudy, Ramakrishna Devananda and Prabhu, K Narayan. "Thermal interface materials for cooling microelectronic systems: present status and future challenges." *Journal of Materials Science: Materials in Electronics* Vol. 32 (2021): pp. 11339–11366.
- [6] Moffat, Robert J. "Describing the uncertainties in experimental results." *Experimental thermal and fluid science* Vol. 1 No. 1 (1988): pp. 3–17.
- [7] Azar, Kaveh. *Thermal measurements in electronics cooling*. CRC press (1997).
- [8] Kozarek, Robert L. "Effect of case temperature measurement errors on the junction-to-case thermal resistance of a ceramic PGA." 1991 Proceedings, Seventh IEEE Semiconductor Thermal Measurement and Management Symposium: pp. 44–51. 1991. IEEE.
- [9] Department of Defense. "MIL-STD-883E, Test Method Standard, Micro-circuits." Method 1014.9. Department of Defense. 1995.
- [10] Standard, JEDEC and Guideline, Two-Resistor Compact Thermal Model. "JESD15-3." (2008).
- [11] SEMI. "G30-88: Specification for Cassette, Shipping and Storage Box for 125mm Bare Wafers." Technical report no. SEMI. 1988.
- [12] Open Compute Project. "Cold Plate Development and Qualification." White paper. Open Compute Project Foundation. 2021. URL https://www.opencompute.org/documents/cold-plate-development-and-qualification.
- [13] Lees, Charles Herbert. "XI. Bakerian lecture.—The effect of temperature and pressure on the thermal conductivities of solids.—Part II. The effects of low temperatures on the thermal and electrical conductivities of certain approximately pure metals and alloys." *Philosophical Transactions of the Royal Society of London. Series A, Containing Papers of a Mathematical or Physical Character* Vol. 208 No. 427-440 (1908): pp. 381–443.
- [14] Prasher, Ravi S. "Surface chemistry and characteristics based model for the thermal contact resistance of fluidic interstitial thermal interface materials." *J. Heat Transfer* Vol. 123 No. 5 (2001): pp. 969–975.

APPENDIX A. UNCERTAINTY PARAMETERS GLOSSARY

TABLE 3: PARAMETERS USED TO COMPUTE THE UNCERTAINTY OF THE THERMAL RESISTANCES.

Sensitivity coefficient	Uncertainty
$\partial R/\partial T_c = 1/Q$	$U_{T_c} = \sigma_{T_c}$
$\partial R/\partial T_{in} = -1/Q$	$U_{T_in} = \sigma_{T_{in}}$
$\partial R/\partial Q = (T_c - T_{in})/Q$	U_Q

TABLE 4: PARAMETERS USED TO COMPUTE THE UNCERTAINTY OF THE HEAT FLOW.

Sensitivity coefficient	Uncertainty
$\partial Q/\partial k = AdT/dy$	U_k =38.2836 Wm ⁻¹ K ⁻¹
$\partial Q/\partial A = k dT/dy$	U_A =3.5355e-8 m ²
$\partial Q / \partial (dT/dy) = kA$	$U_{dT/dy}$, is the standard error corre-
	sponding to the linear regression ap-
	plied to the HFMB temperature mea-
	surements

TABLE 5: PARAMETERS USED TO COMPUTE THE UNCERTAINTY OF THE CASE TEMPERATURE BY USING FOURIER'S LAW.

Sensitivity coefficient	Uncertainty
$\partial T_{c,Fo}/\partial Q = -\Delta y/kA$	U_Q
$\partial T_{c,Fo}/\partial \Delta y = -Q/kA$	$U_{\Delta y}$ =1e-5 m
$\partial T_{c,Fo}/\partial A = Q\Delta y/kA^2$	U_A =3.5355e-8 m ²
$\partial T_{c,Fo}/\partial k = Q\Delta y/k^2 A$	U_k =38.2836 Wm ⁻¹ K ⁻¹
$\partial T_{c,Fo}/\partial T_{Fo,1}=1$	$U_{T_{Fo,1}} = \sigma_{T_{Fo,1}}$